Biospectra : ISSN: 0973-7057, Vol. 20(1), March, 2025, pp. 9-22

An International Biannual Refereed Journal of Life Sciences

Animal Science

ISSN : 0973-7057

In silico characterisation of p62 protein in *Dictyostelium discoideum*: Structural and Functional insights

Saksham Gautam & Shweta Saran*

School of Life Sciences, Jawaharlal Nehru University, New Delhi, India

Orchid Number: SS: 0000-0002-0238-498X

Received : 11th November, 2024 ; Revised : 29th December, 2024

DOI:-https://doi.org/10.5281/zenodo.15731938

Abstract- The p62/SQSTM1 (Sequestosome 1) is a conserved adaptor protein involved in various cellular pathways like selective autophagy, ubiquitin signalling, and protein homeostasis. p62 is extensively studied in higher eukaryotes, while its structural and functional roles in lower eukaryotes remain unclear. This study analyses the p62 homolog of *Dictyostelium discoideum* (*Dd*) through phylogenetic, structural, and domain interaction analysis. Cross-species evolutionary assessment revealed that *Dd*p62 retains key functional domains but exhibits differences in oligomerisation and ubiquitin-binding mechanisms. Using AlphaFold 3-based structural modelling and molecular docking, we accessed and compared the oligomerisation properties of the *Dd*p62-PB1 domain with PB1 domains of higher eukaryotic organisms (*Homo sapiens*, *Rattus norvegicus*). Results show that *Dd*p62-PB1 can form both homo- and heterodimers with a strong affinity than human p62. Similarly, the UBA domain of *Dd*p62 displayed a strong electrostatic binding affinity for ubiquitin, indicating a more rigid and specific interaction, unlike the more flexible ubiquitin recognition in higher eukaryotes. Our findings suggest that p62 functions primarily as an aggregation-prone scaffold protein in lower eukaryotes. At the same time, in higher organisms, it has evolved into a dynamic regulator of selective autophagy and cellular stress responses. This study provides insights into the functional divergence of p62, highlighting its transition from a structural autophagy adaptor to a versatile signalling hub in eukaryotic evolution.

Keywords: p62/SQSTM1, ubiquitin signalling, PB1 oligomerisation, aggregation, *in silico*

INTRODUCTION

Sequestosome 1 (p62/SQSTM1) is a multifunctional adaptor protein involved in selective autophagy, protein degradation, and intracellular signalling pathways. p62 is an evolutionarily conserved protein from Amoebozoa to Metazoa. It plays a crucial role in maintaining proteostasis by bridging ubiquitinated cargo and degradation pathways, including the autophagy and the ubiquitin-proteasome system (UPS).[1] In addition, p62 is also an integral component of stress response pathways (NRF2), NF-κB signalling, and phase separation during protein condensates, showing its broad functional role in cells.[2] This protein is also established as an adaptor in the mitophagy pathway.[3] Recent studies revealed that p62 is a crucial regulator of liver metabolism, and it's impaired function is linked to liver disease progression.[4] It also links cellular defence against oxidative stress and viral pathogenesis.[5] Due to its multifactorial role in the cell, p62-mediated autophagy is also linked to ageing.[6]

Structurally, p62 consists of multiple functional domains that regulate its interactions. Among them, N-

*Corresponding author :
Phone : 9871382398
E-mail : sakshamgautam17@gmail.com
ssaran@mail.jnu.ac.in

terminal Phox and Bem1 (PB1) and C-terminal Ubiquitin-Associated (UBA) are directly involved in the quality control mechanism of cellular proteins. The PB1 domain contains a conserved OPCA (Oligomerization PB1 C-terminal acidic) motif and basic lysine residues, facilitating electrostatic interactions mediating its oligomerisation.[7] Thus, this enables the formation of p62 condensates essential for autophagosome biogenesis and selective autophagy.[8] The hetero-oligomerisation of PB1 domain in higher eukaryotes allows it to interact with other PB1-domain-containing proteins like PKCζ (Protein Kinase Cζ), MEK5 (Mitogen-activated protein kinase kinase 5) and NBR1 (Neighbor of BRCA1 gene 1) regulating NF-κB (Nuclear Factor Kappa-Light-Chain-Enhancer of Activated B Cells) signalling, and cell survival pathways.[9,10] Structural studies have also shown that PB1-mediated oligomerisation amplifies selective degradation pathways by forming higher-order assemblies that cluster ubiquitinated cargo into phase-separated condensates.[11,12] Mutations in the PB1 domain of p62 disrupt its oligomerisation, leading to autophagic defects and accumulation of protein aggregates linked with neurodegenerative diseases (ALS, Parkinson's, and Alzheimer's), Paget's disease of bone[13] and cancer[14], indicating its significance role in maintaining quality control. On the other hand, the Ubiquitin-Associated (UBA) domain, found at the C-terminal end, mediates selective recognition of polyubiquitin chains, directing substrates for degradation via autophagy or the proteasome.[15] The UBA domain has a distinct structural role, containing a conserved hydrophobic patch that specifically binds Lys48- and Lys63-linked polyubiquitin chains.[16] Therefore, mutations in the UBA domain have been strongly implicated in Paget's disease of bone (PDB) and neurodegenerative conditions, where impaired ubiquitin recognition disrupts cellular degradation pathways.[17] Recent crystal structure analyses have revealed that UBA binding to ubiquitin induces a conformational switch, shifting from a dimeric state to a monomeric state, which increases its binding affinity and enables efficient substrate recognition.[18]

The p62 protein as an autophagy adaptor protein was first identified amongst the Amoebozoa group. Few studies in soil amoeba *Dictyostelium discoideum* have experimentally explored the aggregation and ubiquitin-binding properties of p62 homolog in this amoeba.[19,20] Present study aims to examine the primitive form of p62/SQSTM1 protein in *Dictyostelium discoideum* to understand the evolutionary and mechanistic insights into its role during cellular homeostasis. This study employs computational approaches for the comparative assessment of structural and evolutionary features and functional interactions of the *Dictyosteium* p62 protein. Due to the unavailability of the experimentally resolved 3D structure of *Dictyosteium* p62 (*Dd*p62) and higher disordered regions, we have utilised novel diffusion-based deep learning to predict high-quality structures of conserved PB1 and UBA domains using AlphaFold 3 server.[21] Generated models were refined using molecular dynamic simulations (MD simulations) and assessed RMSD (root mean square deviation), RMSF (root mean square fluctuation), and Rg (radius of gyration). Refined 3D models were then utilised for protein-protein docking and detailed assessment of the interaction interface of protein complexes to identify the interacting residues, type of interactions involved and overall complex stability. This study uncovers the crucial structural features of *Dictyostelium* p62 protein and its functional divergence from complex organisms to get clearer insights into the key functions of p62 protein.

MATERIALS & METHODS

Sequence retrieval and construction of phylogenetic tree

The p62/SQSTM1 protein sequence of *Dictyostelium discoideum* was retrieved from dictyBase.org (http://www.dictybase.org). p62 homologue protein sequences of human (*Homo sapiens*; sqstm1), mouse (*Mus musculus*; sqstm1), *Drosophila melanogaster* (Ref (2)P), *Danio rerio* (sqstm1) *and Caenorhabditis elegans* (sqst1) were obtained from UniProt databse (http://www.uniprot.org/uniprotkb).[22] Retrieved sequences were imported to Molecular Evolutionary Genetics Analysis Software (MEGA11)[23] and aligned by multiple sequence alignment, and a phylogenetic tree was constructed using the maximum likelihood tree method. Evolutionary relationships between different orthologs were identified using the OrthoDB database.[24]

Identification of conserved domains, motifs and interacting proteins

To identify the conserved domains in p62 protein, the protein sequences of *Homo sapiens* p62 (*Hs*p62) and *Dictyostelium discoideum* p62 (*Dd*p62) were subjected to InterPro 104.0 and conserved domains were identified.[25]

Conserved motifs across p62 protein sequences were identified using MEME (Multiple Em for Motif Elicitation) [26]motif discovery tool 5.5.7 by selecting discriminative

search mode and for 10 motifs per sequence. The protein sequence of *Hs*p62 was taken as a control for motif discovery.

Functional protein association networks of *Dd*p62 and *Hs*p62 were prepared using the STRING [27] tool (https://string-db.org). An evidence-based full-string network was accessed with medium confidence (0.400) and 10 maximum interactors in the first shell. Gene ontology-based functional enrichment was also analysed for the p62 protein in the analysis tab of STRING.

Tertiary structure prediction and refinement

For 3D structure prediction of different domains, a sequence of specific domain was retrieved from the UniProt database and subjected to the AlphaFold 3 server with default parameters. Alphafold- 3 uses diffusion-based deep learning to predict biomolecule structures using a pair former module.[21] Alphafold generated five high-scoring models, and the quality of the generated models was then accessed based on the pLDDT (per-atom confidence) and pTM (predicted template modelling score) scores.

The stability of these generated 3D models was checked by molecular dynamics simulations in the WebGrow-UAMS server (https://simlab.uams.edu) using the GROMACS with the GROMOS96 43a1 force field.[28] The complexes were solvated using a simple point charge (SPC) water model in a triclinic box with the addition of 0.15M NaCl. Five thousand energy minimisation steps were employed using the steepest descent approach. After that, the system was subjected to NVT/NPT equilibration at 298 K temperature and 1 bar pressure, followed by a production run of 50 ns for 5000 frames per simulation. Resulted parameters, including Root Mean Square Deviation (RMSD), Radius of Gyration (Rg), and Root Mean Square Fluctuation (RMSF), were analysed. After the MD run, 3D models were refined using the GalaxyRefine tool[29] in the GalaxyWEB server (https://galaxy.seoklab.org). Most stable models were selected to generate a complete PROCHECK analysis[30] in the PDBsum database[31] to get the Ramachandran plot for the 3D model.

Protein-protein docking and complex refinement

The template-based protein-protein docking was performed using the Homomer[32] and Heteromer[33] tools in the GalaxyWEB server. It uses template-based assembly to predict homomer and heteromer and performs *ab initio* docking if a template is unavailable. Generated models were arranged based on interface area and template similarity. *Ab initio* rigid body docking was performed using GalaxyTongDock[34] which is a program to dock heteromeric proteins.

The docked protein-protein complexes were further refined using the Refinement tool in HADDOCK 2.4 (https://rascar.science.uu.nl/haddock2.4).[35] As a result, top-scoring complexes were generated and ranked based on the weighted sum of different energy, which was named The HADDOCK score.[36] The HADDOCK scoring function can be described as the below equation:

$$\text{HADDOCK score} = 0.2 \times E_{vdw} + 1.0 \times E_{elec} + 1.0 \times E_{desolv} + 0.1 \times E_{AIR}$$

Where E_{vdw} is the van der Waals energy, E_{elec} denotes the electrostatic energy, E_{desolv} represents the desolvation energy, and E_{AIR} represents the ambiguous interaction restraints energy.

Analysis of protein-protein interface

The interaction interface in a complex was analysed using the PDBsum Generate tool (https://www.ebi.ac.uk/thornton-srv/databases/pdbsum/Generate.html).[31] The protein-protein interaction interface, representing key interacting residues involved was analysed. Cartoon representations of the protein complexes, highlighting polar interactions, were generated using PyMOL (Schrödinger, LLC).

RESULTS & DISCUSSION

Phylogenetic analysis of p62 protein

For comparative analysis of the phylogeny of p62 protein, sequences of p62 proteins of model organisms across different species (*Dictyostelium discoideum, Drosophila melanogaster, Caenorhabditis elegans, Danio rerio, Mus musculus, Homo sapiens)* were retrieved, and multiple sequence alignment was performed using ClustalW, and a phylogenetic tree was constructed using MEGA11. The phylogenetic tree [Figure 1.A] illustrates the evolutionary relationships of the SQSTM1 (Sequestosome-1) proteins across different species, highlighting varying degrees of divergence. The closest relationship was observed between the p62 protein from *Homo sapiens* (human), *Mus musculus* (mouse) and *Danio rerio* (zebrafish) (evolutionary distance < 0.5). In contrast, the p62 ortholog in *Drosophila melanogaster* (Ref(2)P) exhibits greater divergence. The most significant evolutionary distances were observed in Caenorhabditis elegans (nematode) and *Dictyostelium discoideum* (slime mould), which exhibit a primitive form of p62 protein in lower eukaryotes. The tree shows that SQSTM1 homologs

are highly conserved in vertebrates (humans, mice, zebrafish) and have diverged more significantly in invertebrates (*Drosophila, Caenorhabditis*) and protists-(*Dictyostelium*). It indicates that p62-like proteins existed in early eukaryotes and evolved separately in different lineages.

Orthology search by OrthoDB indicated the first appearance of the SQSTM1 orthologs in Amoebozoa (*Dictyostelium*) [Figure 1.C]. In contrast, another well-characterised autophagy adaptor protein, the NBR1 orthologs, shows sign of first appearance in Red Algae (*Rhodophyta*) [Figure 1.B]. Functionally, the most evolved or specialised forms of NBR1 and p62 is present among fungi and metazoa. From these results, we can predict that the origin of Selective Autophagy Receptors (SARs) may be linked to *Dictyostelium,* which has evolved functionally in different species. Although phylogenetic tree analysis predicted *Caenorhabditis elegans* as the most primitive and distantly related form of p62, it could probably be due to any domain loss or rapid sequence divergence in the p62 homolog of *Caenorhabditis elegans.*

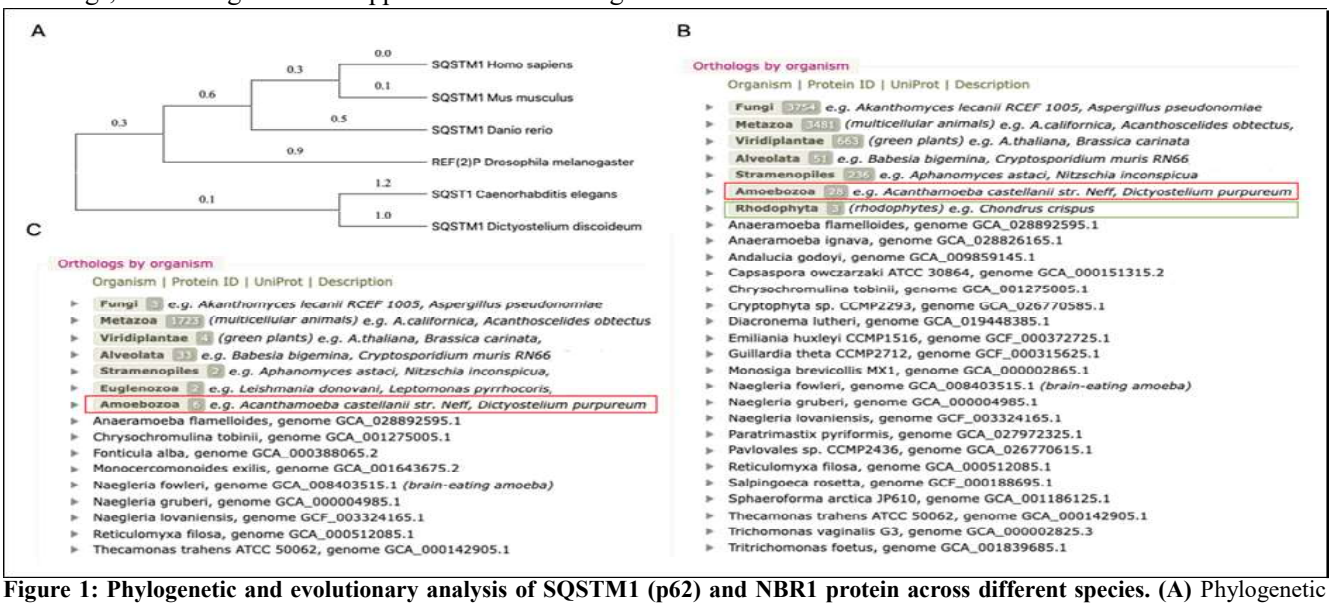

Figure 1: Phylogenetic and evolutionary analysis of SQSTM1 (p62) and NBR1 protein across different species. (A) Phylogenetic analysis of p62 protein across different organisms generated by MEGA11 tool using maximum likelihood method and ClustalW was used as multiple sequence alignment tool. Branch lengths indicating the degree of divergence. The highest evolutionary distance is observed for *C. elegans* and *Dictyostelium discoideum*. The tree includes sequences from: *Homo sapiens* (Uniprot ID: Q13501), *Mus musculus* (Uniprot ID: Q64337), *Danio rerio* (Uniprot ID: Q6NYK8), *Drosophila melanogaster* (Ref(2)P, Uniprot ID: P25006), *Caenorhabditis elegans* (Uniprot ID: Q20967), *Dictyostelium discoideum* (Uniprot ID: Q54PS8). Orthology analysis of **(B)** *NBR1* and **(C)** *SQSTM1 (p62)* genes, showing their presence across different taxonomic groups based on OrthoDB data. The proteins are conserved in fungi, metazoans, plants, and amoebozoa, suggesting an ancient origin and functional divergence. OrthoDB search results show the origin and diversification of the p62 ortholog from Amoebozoa (highlighted in red box) and NBR1 ortholog from Rhodophyta (highlighted in green box).

Identification and functional analysis of conserved domains and motifs

Domains are independent structural and functional units of a protein that can fold and operate autonomously, while the motifs are short, conserved sequence patterns that are often present within domains and contribute to specific functional properties. Domains and motifs are crucial in determining a protein's function and evolution. To investigate the conservation of these structural elements, conserved domains in *Homo sapiens* (*Hs*p62) [Figure 2.A(i)] and *Dictyostelium discoideum* (*Dd*p62) [Figure 2.A(ii)] were identified using InterPro 104.0.[25] Results from InterPro showed that the three major domains- Phox and Bem1 (PB1), Zinc Finger (ZZ), and Ubiquitin-Associated Domain (UBA) were conserved from *Dictyostelium* to *Homo sapiens*, suggesting their fundamental role in cellular processes. An NBR1-like domain was also identified in *Dd*p62, located downstream of the Zinc Finger domain, indicating potential functional divergence of p62 while maintaining core regulatory mechanisms. Along with these, *Dd*p62 have more intrinsically disordered regions dispersed across the protein.

To examine the presence of conserved motifs, the MEME Motif Discovery tool was used in MEME Suite 5.5.7,[26] with *Hs*p62 protein as a reference. The analysis identified 10 motifs [Figure 2. B] in *H. sapiens* and *Mus*

musculus (*Mm*p62), while *Danio rerio* (*Dr*p62) contained six motifs. A gradual reduction was observed in *Drosophila melanogaster* (*Dm*p62), *Caenorhabditis elegans* (*Ce*p62), and *Dictyostelium discoideum* (*Dd*p62), which exhibited only 3, 1, and 2 motifs, respectively. Among them, a motif within the ZZ domain was the only one consistently found across all species, including *Dictyostelium*, emphasising its essential function. In contrast, a motif containing the LIR (LC3-interacting region) sequence was exclusively detected in *H. sapiens*, *M. musculus*, and *D. rerio*, likely due to more significant evolutionary divergence of these vertebrates from lower eukaryotes. Motif search results showed that *Dd*p62 and *Ce*p62 have the highest p-values of 3.55e-35 and 1.94e-21, respectively, showing the weakest conservation of motifs.

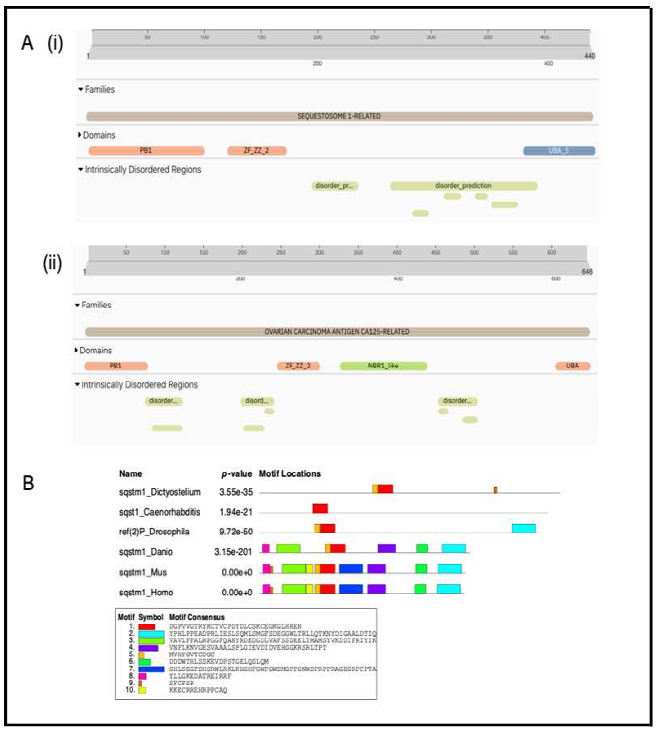

Figure 2: Comparative domain architecture and motif analysis of SQSTM1 across species (A) Domain organisation of SQSTM1 protein of **(i)** *Homo sapiens* and **(ii)** *Dictyostelium discoideum*. The conserved protein domains, including PB1 (Phox and Bem1 domain), ZF_ZZ_2 (zinc finger domain), and UBA (ubiquitin-associated domain), are highlighted in different colours with intrinsically disordered regions marked in green. **(B)** Conserved motif analysis of SQSTM1 across different species, including *Caenorhabditis elegans*, *Drosophila melanogaster*, *Danio rerio*, *Mus musculus* and *Homo sapiens* using the MEME Suite. The presence and location of conserved motifs are represented by colour bars along with their respective p-values. Sequences of the identified motifs are provided in the inset. The p-values indicate the statistical significance of conserved motifs, with the highest values in *Caenorhabditis elegans* and the lowest values in *Mus musculus* and *Homo sapiens*.

As observed, the presence of several conserved domains and motifs in *Hs* p62 is the key factor behind its diverse functionality across multiple cellular pathways. Among identified domains, the PB1 domain mediates homo or hetero-oligomerisation with other signalling proteins, enabling p62 to form protein aggregates during autophagy.[8] Another key domain, the ZZ-type zinc finger, binds with RIPK1 (Receptor-interacting serine/threonine-protein kinase 1), regulating NF-κB signalling.[37] The C-terminal UBA domain is responsible for the binding of ubiquitinated proteins.[15] The KEAP1-interacting region (KIR motif) enables the interaction of p62 with KEAP1, leading to Nrf2 activation and antioxidant response,[38] while the TRAF6-binding motif links p62 to NF-κB signalling.[39] The LC3-interacting region (LIR motif), a short-conserved sequence (WXXL/I/V), facilitates binding to LC3 and GABARAP family proteins of the autophagosome, allowing p62 to function as an autophagy adaptor.[1,40] Like many motifs, the LIR motif (represented by a dark green bar at C-terminal of proteins in Figure 2.B) was also absent in *Ce*p62, *Dm*p62 and *Dd*p62, indicating their higher evolutionary divergence. The *Cep*62 has the highest p-value for conserved motifs, suggesting a higher likelihood of domain loss or rapid evolutionary changes.

To understand the functional interaction enrichments of *Dd*p62, we compared the STRING interaction networks of *Dd*p62 with *Hs*p62. In the STRING results, *Hs*p62 [Figure 3. A(i)] was found to interact with LC3 proteins (MAP1LC3A and MAP1LC3B) and the GABARAP family proteins (GABARAP, GABARAPL1, and GABARAPL2), which are essential for autophagosome formation and maturation. Additionally, *Hs*p62 interact with UBC (Ubiquitin C), reinforcing its role in targeting misfolded proteins for degradation. Another notable interaction was with NBR1, an autophagy adaptor known for oligomerising with p62. Furthermore, interactions of *Hs*p62 with TRAF6 (TNF receptor-associated factor 6), KEAP1 (Kelch-like ECH-associated protein 1), and RIPK1 (Receptor-interacting protein kinase 1) reaffirmed its involvement in NF-κB signalling, Nrf2-mediated oxidative stress response, and cell death pathways, respectively. Due to its multiple interacting partners, *Hs*p62 functions as a signalling hub rather than solely an autophagy adaptor, as the domains and motifs facilitating these interactions are well-conserved across metazoans. On the other hand, *Dd*p62 [Figure 3. A(ii)] exhibited strong associations with ubiquitin proteins (UbqB, UbqC, UbqO, and UbqP) and

autophagic components such as Atg8 (LC3 homolog in *Dictyostelium*). It also interacted-with an uncharacterised PB1 domain-containing protein (DDB0185872; hereafter, *Dd*X), suggesting the presence of another adaptor protein. It shows that some interactions of PB1 domain (oligomerisation with another PB1-containing protein) and UBA domain (with ubiquitin molecules) are conserved from *Dictyostelium* to *Homo sapiens,* suggesting functional similarity. Unlike *Hs*p62, *Dd*p62 lacks direct connections to oxidative stress regulators, cell-death components, and NF-κB pathway elements, indicating a more targeted function in proteostasis and autophagy rather than complex signalling. Gene Ontology (GO) enrichment analysis [Figure 3.B] further supports this distinction, predicting the involvement of *Dd*p62 in cellular catabolic processes and the macro-autophagy pathway, with at least 80% group similarity and the highest statistical significance (False Discovery Rate ~ 1.0e-05 and ~ 7.0e-05). These findings suggest that while *Hs*p62 has evolved into a multifunctional signalling hub, *Dd*p62 primarily specialized in proteostasis and autophagy, reflecting evolutionary divergence in its functional roles.

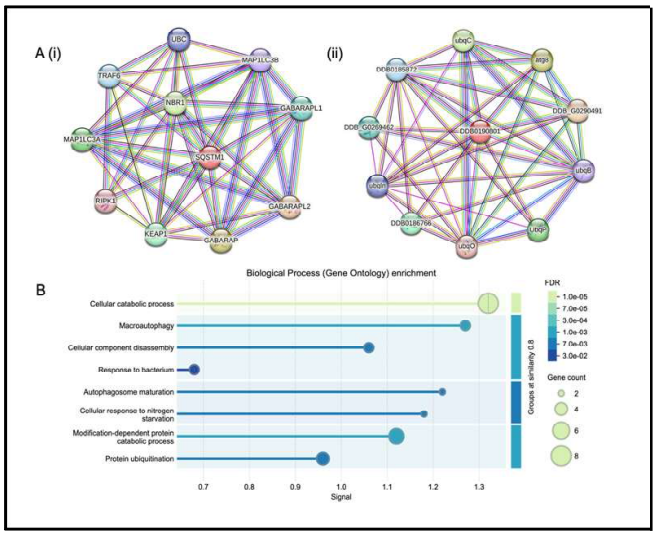

Figure 3: Comparative analysis of interaction network and functional enrichment of SQSTM1 protein of *Homo sapiens* and *Dictyostelium discoideum*. (A) Protein-protein interaction networks of **(i)** SQSTM1 (p62) in *Homo sapiens* and **(ii)** its homolog in *Dictyostelium discoideum* (identifier: DDB0190801), generated using the STRING database. Nodes represent proteins, and joining lines indicate interactions, with different colours representing various interactions. In the STRING network, blue lines represents known interactions from the curated databases, pink/red indicates experimentally determined interactions, green shows predicted interactions from gene neighbourhood, light blue/cyan represents gene co-occurrence, black indicates co-expression, purple signifies interactions based on protein homology, and yellow is derived from text mining. **(B)** Gene Ontology (GO) enrichment analysis of SQSTM1 of *Dictyostelium discoideum,* showing associated biological processes. The X-axis represents the enrichment signal, while the Y-axis lists the associated biological processes, including macroautophagy, protein ubiquitination and response to starvation. The size of the circles corresponds to the involved gene count, and the colour gradient indicates the False Discovery Rate (FDR), with lighter shades representing lower FDR values.

Tertiary structure prediction of desired domains

The tertiary structure of a protein is crucial for understanding its function, stability, and interactions. Since structure defines how a protein binds to partners and carries out biological activities, modelling provides deeper insights into its functional mechanisms. Therefore, to understand better the functional relevance of p62 protein in *Dictyostelium*, we predicted the tertiary structures of PB1 domain, UBA domain of *Dd*p62 and PB1 domain of p62 interacting protein (identified interacting partner from STRING database) based on diffusion-based deep learning architecture using AlphaFold 3 server.[41] [Figure 4]

The quality of modelled structures was determined based on pLDDT and pTM scores, which show the local residue-level confidence and overall global fold reliability, respectively. All three structures showed maximum residues having very high confidence scores (pLDDT > 90) and some residues in high confidence regions (90 > pIDDT > 70), indicating high-quality prediction. However, the structure of the PB1 domain from uncharacterised protein

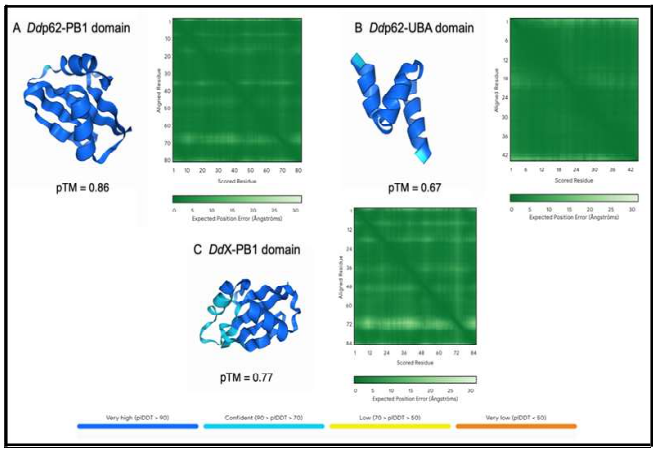

Figure 4: 3D structure prediction and confidence assessments of different domains of *Dd*p62 and uncharacterised PB1 containing protein from *Dictyostelium discoideum*. Figure shows the structural models and confidence scores for **(A)** PB1 domain of *Dd*p62, **(B)** UBA domain of *Dd*p62, and **(C)** PB1 domain of the uncharacterised protein (*Dd*X; DDB0185872). Models are colour-coded based on pLDDT confidence scores, depicted in the lower bar and heatmap showing the expected positional error for aligned residues (in Å) in predicted models.

showed a region with high flexibility between residue 60 and 80. Most predicted structures have a pTM score of 0.7 or higher, indicating high confidence in their global fold accuracy. In contrast, one model (UBA domain) with a pTM of 0.67 suggests slightly lower but reasonable structural reliability [Figure 4B]. A top-scoring model was selected for further analysis among the predicted model clusters for each domain. The tertiary structures of the UBA domain of *Homo sapiens* (*Hs*p62, PDB; 2JY8)[42] and the ubiquitin monomer from *Homo sapiens* (*Hs*UB, PDB; 1UBQ)[43] were retrieved from the Protein Data Bank (PDB).

Structure refinement and validation

The stability and flexibility of all protein structures (predicted models and obtained from PDB) were analysed through fully solvated Molecular Dynamics (MD) simulations conducted for 50 ns using the GROMACS in the WEBGROW server.[44,45] The key parameters, such as RMSD, Rg, and RMSF, [Figure 5] were evaluated to assess the structural quality of each domain. Root Mean Square Deviation (RMSD) represents protein structural stability and conformational changes over time. The RMSD values for *Dd*p62-PB1 and *Dd*X-PB1 [Figure 5A(i) and C(i)] remained within the ranges of 0.1–0.25 nm and 0.1–0.4 nm, respectively, indicating minimal structural deviations throughout the simulation. Conversely, the *Dd*p62-UBA domain exhibited a sharp increase in RMSD during the first 10 ns, reaching approximately 0.4 nm before stabilizing around 0.5–0.6 nm, probably due to conformational shifts and its structural flexibility [Figure 5B(i)]. The RMSF value of a protein represents the residue-level flexibility of the structure. RMSF analysis of *Dd*p62-UBA confirmed a significant fluctuation in different regions of the protein [Figure 5B(ii)] with a considerable fluctuation at the C-terminal region (~0.5 nm), suggesting possible unfolding or increased flexibility. In the *Dd*p62-PB1 domain, a notable peak (~0.45 nm) was observed at residue ~45, showing a flexible region [Figure 5A(ii)]. Similarly, in the PB1 domain of the *Dd*X protein, two prominent peaks were identified at residues 40 and 50, along with a minor peak around residue 70, indicating the dynamic behaviour of the protein [Figure 5C(ii)].

The Radius of Gyration (Rg) shows the compactness of a protein during simulation. The Rg values remained relatively stable in the *Dd*p62-PB1 domain, while the PB1 domain of the *Dd*X protein showed initial fluctuations but stabilised after 10 ns, with values around 1.18–1.20 nm [Figure 5A(iii) and 5C(iii)]. The *Dd*p62-UBA domain exhibited more noticeable fluctuations [Figure 5B(iii)], with Rg values ranging between 0.95 and 1.05 nm, suggesting greater flexibility. Therefore, MD results indicate that the PB1 domain of *Dd*p62 is the most stable and compact, while the PB1 domain from the uncharacterised protein demonstrates intermediate stability with some flexible regions. In contrast, the UBA domain appears to be the least stable, likely undergoing significant conformational rearrangements as observed in the *Hs*p62-UBA domain.[42]

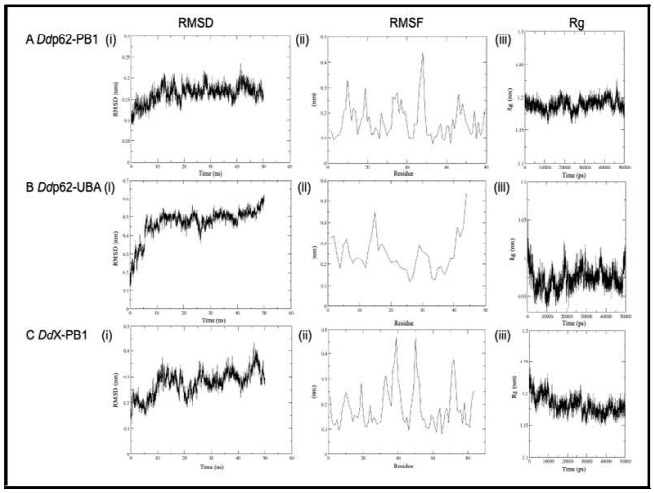

Figure 5: Structural stability and conformational dynamics of predicted domain structures in MD simulation. Graphical representation of **(i)** RMSD, **(ii)** RMSF, and **(iii)** Rg (y-axis) values of the backbone atoms from **(A)** *Dd*p62-PB1, **(B)** *Dd*p62-UBA, and **(C)** *Dd*X-PB1 (PB1 domain of uncharacterized protein) protein structures.

All three predicted domain structures were further refined using the Refine tool from the GalaxyWEB server. GalaxyRefine optimizes side-chain conformations using a rotamer library and refines the backbone structure, generating multiple refined models and ranking them based on stability and quality metrics. Based on the Ramachandran plot, high-quality, stable models were selected and analyzed using PDBsum for PROCHECK validation. The PROCHECK confirms high structural quality for all three domain statistics. The *Dd*X-PB1 domain showed 97.4% of residues in the most favoured regions, indicating a highly stable structure. The *Dd*p62-PB1 and *Dd*p62-UBA domains had 90.8% and 92.3% residues in the most favoured region, respectively, with the rest in allowed regions (data not shown). This suggests good stability, though they exhibit slightly more structural flexibility than *Dd*X-PB1. All three domains structures exceed the 90% threshold, making them suitable for protein-protein docking.

Molecular docking and refinement of protein complexes

The p62 protein plays a vital role in forming ubiquitinated protein aggregates and also facilitates their removal through the selective autophagy pathway. Its N-terminal PB1 and C-terminal UBA domains, along with the LIR motif, are crucial for this process. The PB1 domain mediates homo- or hetero-oligomerisation of p62, while the UBA domain binds with the ubiquitin-tagged proteins, leading to the formation of cytosolic aggregate. The autophagy machinery then recognizes and degrades these ubiquitinated aggregates, ensuring cellular protein homeostasis. To explore the functional significance of *Dd*p62, we analysed its PB1 domain interactions for homo- or hetero-oligomerisation and its UBA domain binding with the ubiquitin monomer from *Homo sapiens* to understand its affinity for ubiquitinated proteins. The GalaxyHomomer tool on the GalaxyWEB server predicted *Dd*p62-PB1 homo-oligomer structures by identifying structural templates and applying *ab initio* blind docking for structure generation and refinement. Similarly, GalaxyHeteromer was used to predict hetero-oligomers of *Dd*p62-PB1 and *Dd*X-PB1, following the same approach. The Galaxy Homomer tool predicted five homodimer complexes for *Dd*p62-PB1, of which four were template-based docking structures, and one was generated using an *ab initio* docking approach. Similarly, the GalaxyHeteromer tool identified the same template structure for heterodimer prediction of *Dd*p62-PB1 and *Dd*X-PB1. In both cases, the template suggested by GalaxyWEB corresponded to the crystal structure of a PB1 domain complex of Protein Kinase C iota and Par6 alpha from *Homo sapiens*[46], which was selected as a reference complex for studying interactions. Unlike Galaxy Homomer, GalaxyHeteromer does not generate *de novo* docked complexes, likely due to its limitation in creating entirely new heteromeric structures. Therefore, *ab initio* docking of *Dd*p62-PB1 with *Dd*X-PB1 was performed using GalaxyTongDock, a rigid-body docking web server. Similarly, the docking of *Dd*p62-UBA and *Hs*p62-UBA with human ubiquitin (*Hs*-Ub) was conducted using the same approach. From GalaxyTong Dock results, the complex with the largest cluster size and highest docking scores was selected for further refinement.

The selected protein complexes were then refined using the explicit solvent refinement protocol of the HADDOCK2.4 server. In this protocol, protein complexes first undergo semi-flexible refinement to allow conformational adjustments and energy minimisation, followed by short molecular dynamics simulations to remove the hindrance from steric clashes and optimised hydrogen bonding.

Analysis of the top-scoring clusters (Table 1) revealed that among the *Dictyostelium* PB1 homodimers, the *de novo* docked *Dd*p62-PB1 homodimer exhibit the lowest HADDOCK score (-154.5 ± 3.8), indicating a highly favourable binding. This claim was further supported by strong electrostatic interactions (-701.8 ± 21.3), suggesting a more stabilized complex. Similarly, among the *Dd*p62-PB1 heterodimers, the *de novo* docked complex showed higher stability than the homology-based docked complex with a significantly lower HADDOCK score (-117.4 ± 2.8) and stronger binding interactions. Although *de novo* docked *Dd*p62-PB1 heterodimer has slightly higher desolvation energy (25.5 ± 0.8) than homology based complex, but it could not overshadow the overall binding strength of the complex. These observations indicate that the *de novo* docked PB1 complexes displayed higher stability, probably making them closer to the actual complexes. In the overall comparison of PB1 interaction, the PB1 homodimer exhibit a higher HADDOCK score than the heterodimer (-154.5 ± 3.8 vs -117.4 ± 2.8) along with the stronger electrostatic interactions, indicating a more favourable and stable binding. In the p62UBA-ubiquitin (Ub) interaction, the *Dd*p62UBA-Ub complex demonstrated a higher HADDOCK score (-95.5 ± 4.9) than *Hs*p62UBA-Ub (-85.8 ± 0.9), predicting higher stability of the complex. *This could be due to the* more substantial electrostatic energy (-351.9 ± 10.5 vs -121.9 ± 7.3) of the *Dd*p62UBA-Ub complex. While the *Hs*p62UBA-Ub complex exhibits higher van der Waals energy (-63.1 ± 1.7 Vs -33.8 ± 2.8) and lower desolvation energy (1.7 ± 1.2 Vs 8.7 ± 2.6), making it more relied on hydrophobic interactions for its stability but overall *Dd*p62UBA-Ub complex was more stable and energetically favourable.

From these findings, we can say that in *Dicyostelium,* p62 homodimer formation is energetically more favourable than heterodimers, which could explain its aggregation properties.[19] The *Dictyostelium* p62 possesses a Type I/II PB1 domain, allowing it to self-oligomerise and interact with Type I PB1 domains. It could be the reason behind its strong ability of homo- and hetero-oligomerization. This contrasts with human p62, which has a strictly Type I PB1 domain, relying on heterotypic interactions for functional

regulation.[47,48] Similarly, the interaction of the UBA domain of *Dd*p62 with ubiquitin is more efficient than its human homolog, suggesting functional differences in ubiquitin recognition and binding across species. These differences highlight evolutionary variations in ubiquitin-binding efficiency between the UBA domains, surprisingly, with *Dd*p62UBA potentially more optimised for stronger interactions than *Hs*p62UBA.

Table 1: HADDOCK refinement scores and interaction energies of protein complexes.

Protein complex	HADDOCK Score	RMSD (Å)	Van der Waals Energy	Electrostatic Energy	Desolvation Energy
*Dd*p62-PB1 Homodimer (*de novo* docked)	-154.5 ± 3.8	0.5 ± 0.3	-30.9 ± 1.2	-701.8 ± 21.3	16.8 ± 1.8
*Dd*p62-PB1 Homodimer (Homology based)	-85.3 ± 6.0	0.5 ± 0.3	-36.0 ± 2.0	-328.4 ± 20.5	16.4 ± 1.8
Dd-PB1 Heterodimer (Homology based)	-117.4 ± 2.8	0.6 ± 0.3	-36.2 ± 1.5	-533.4 ± 17.2	25.5 ± 0.8
Dd-PB1 Heterodimer (*de novo* docked)	-85.8 ± 1.5	0.5 ± 0.3	-28.6 ± 2.4	-388.6 ± 11.3	20.4 ± 3.3
*Hs*p62UBA-Ub	-85.8 ± 0.9	0.6 ± 0.3	-63.1 ± 1.7	-121.9 ± 7.3	1.7 ± 1.2
*Dd*p62UBA-Ub	-95.5 ± 4.9	0.5 ± 0.3	-33.8 ± 2.8	-351.9 ± 10.5	8.7 ± 2.6

Domain interaction analysis

Interactions in a protein-protein or protein-ligand complex directly influence its conformational and functional properties by determining binding affinity, specificity, and structural stability. Hydrophobic interactions drive protein folding and interface stabilisation, while hydrogen bonds contribute to structural integrity and specificity. Van der Waals forces assist in molecular packing; salt bridges ensure electrostatic stability, and disulfide bonds reinforce structural rigidity, collectively maintaining the stability and functionality of the complex.[49] In this study, we have tried to functionally characterise the interactions of PB1 and UBA domains of *Dictyostelium* p62 based on key structural features. To do that, we retrieved 3D structures of *Hs*p62PB1-homodimer (PB1 homo-dimer from *Homo sapiens* p62, PDB;6JM4)[50], *Hs*PKCi-Par6α-PB1-heterodimer (PB1 domain complex of Protein Kinase C iota and Par6 alpha of *Homo sapiens*, PDB;1WMH)[51], *Rn*p62PB1-homodimer (p62 PB1 dimer of *Rattus norvegicus*, PDB; 2KTR)[52], from Protein Data Bank (PDB database).

All protein complexes (docked and retrieved from PDB) were subjected to a Protein database (PDBsum) to access interactions among key residues (Table 2). These protein complexes were further subjected to the GETAREA web server to identify the Solvent Accessible Surface Area (SASA) for the given complex (Table 3). The solvent-accessible surface area plays a critical role in stability, as a larger SASA generally corresponds to a more exposed interface, requiring stronger stabilising interactions to maintain structural integrity.[53] The known 3D structures of protein complexes were used as a reference for comparative analysis of complex interfaces. Among the PB1 homodimers, the *Dd*p62PB1 homodimer [Figure 6A,F] formed 14 hydrogen bonds and seven salt bridges (Table 2) involving Lys 5, Glu 46, and Arg 74 with a total SASA of 8786.26 Å². In contrast, the *Hs*p62PB1 homodimer [Figure 6B] has the highest SASA among homodimers (8872.33 Å²) (Table 3) but forms only four hydrogen bonds and salt bridges. It relied more on hydrophobic interactions, making it structurally weaker than *the Dd*p62PB1 homodimer. The *Rn*p62PB1 homodimer [Figure 6C] showed a significantly larger SASA of 12030.60 Å², indicating a lesser buried interface, but forms six hydrogen bonds and salt bridges, including strong ASP-ARG ionic interactions, contributing to moderate stability despite its expansive surface. These observations highlight that PB1 domain-mediated homodimerization is primarily stabilized by electrostatic interactions, with Lys 7 and Asp residues being the most conserved. However, species-specific variations in charged and hydrophobic residues, such as Glu 46 (*Dd*p62), Arg 94 (*Rn*p62), and Tyr 89 (*Hs*p62), indicate evolutionary modifications that influence stability and oligomerisation tendencies.

Table 2: Analysis of protein-protein interface interactions using PDBsum.

Complex	Hydrogen Bonds	Non-bonded Contacts	Salt Bridges	Total Interactions
*Dd*p62PB1 Homodimer	14	99	7	120
*Rn*p62PB1 Homodimer	6	43	6	55
*Hs*p62PB1 Homodimer	4	63	4	71
*Dd*p62PB1 Heterodimer	16	91	5	112
*Hs*PB1 Heterodimer	10	84	7	101
*Dd*p62UBA-Ub Complex	8	74	4	61
*Hs*p62UBA-Ub Complex	8	101	-	109

Table 3: Solvent Accessible Surface Area (SASA) of polar and apolar residues calculated using the GetArea server.

Complex	Polar area (Å²)	Apolar area (Å²)	Total area (Å²)
*Dd*p62PB1 Homodimer	3616.72	5169.54	8786.26
*Rn*p62PB1 Homodimer	5248.79	6781.81	12030.6
*Hs*p62PB1 Homodimer	3155.46	5716.88	8872.33
*Dd*p62PB1 Heterodimer	3455.62	5262.9	8718.52
*Hs*PB1 Heterodimer	3850.26	5501.31	9351.57
*Dd*p62UBA-Ub	3042.59	4104.33	7146.92
*Hs*p62UBA-Ub	3117.83	4475.94	7593.77

Among the PB1 heterodimers, the *Dd*p62PB1 heterodimer [Figure 6D, G] achieves strong stability through a dense hydrogen bonding network (16 hydrogen bonds) and five salt bridges, with Glu 47 being the critical residue in polar interactions. The *Hs*p62PB1 heterodimer [Figure 6E] has a larger SASA (9351.57 Å²) than the *Dd*p62PB1 heterodimer, forming 10 hydrogen bonds and seven salt bridges. This higher solvent exposure and fewer hydrogen bonds suggest a less stable complex than the *Dd*p62PB1 heterodimer. However, Glu, Arg, and Lys residues are involved in complex stabilization in both complexes.

On the other hand, in UBA domain interaction with ubiquitin monomer, the *Dd*p62UBA- Ub complex showed higher stability than *Hs*p62UBA-Ub with higher interface area and lower solvent accessibility (SASA value, 7146.92). The interface of *the Dd*p62UBA-Ub complex [Figure 7A,C] has four salt bridges, eight hydrogen bonds, and 74 non-bonded hydrophobic contacts. The *Hs*p62UBA- Ub Complex [Figure 7B,D] has a higher solvent accessible area (7593.77 Å²) with a similar number of hydrogen bonding but much higher hydrophobic (van der Waals) interactions, making it less stable. Both of these UBA domains share conserved key residues Asn44 (*Hs*p62) and Asn60 (*Dd*p62) involved in hydrogen bonding and interface stabilisation; however, *Dd*p62UBA-Ub exhibits stronger electrostatic interactions with Glu64, His68, whereas *Hs*p62UBA-Ub relies more on hydrophobic and polar interactions of Pro21, Ser43.

These results suggest that p62/SQSTM1 has undergone functional adaptations across the evolution. PB1 domain in *Dictyostelium* p62 protein is more specialised for oligomerisation because of its stronger electrostatic interactions and a more rigid structural framework.[54] In contrast, human PB1-mediated interactions appear more dynamic, likely allowing for greater regulatory control over autophagy and signal transduction rather than stable and rigid polymerisation. The evolutionary transition from Type I/II to Type I PB1 domains in higher eukaryotes supports this phenomenon of functional shift from rigid oligomerisation (structural role) to dynamic signalling scaffolding (functional adaptation in autophagy).[48] Similarly, the UBA domain in *Dictyostelium* exhibits a more electrostatically driven interaction with ubiquitin [Figure 7A], whereas the human UBA domain has evolved to accommodate a broader and more transient binding profile [Figure 7B]. This functional shift in humans may be linked to the ability of p62 UBA to recognise diverse

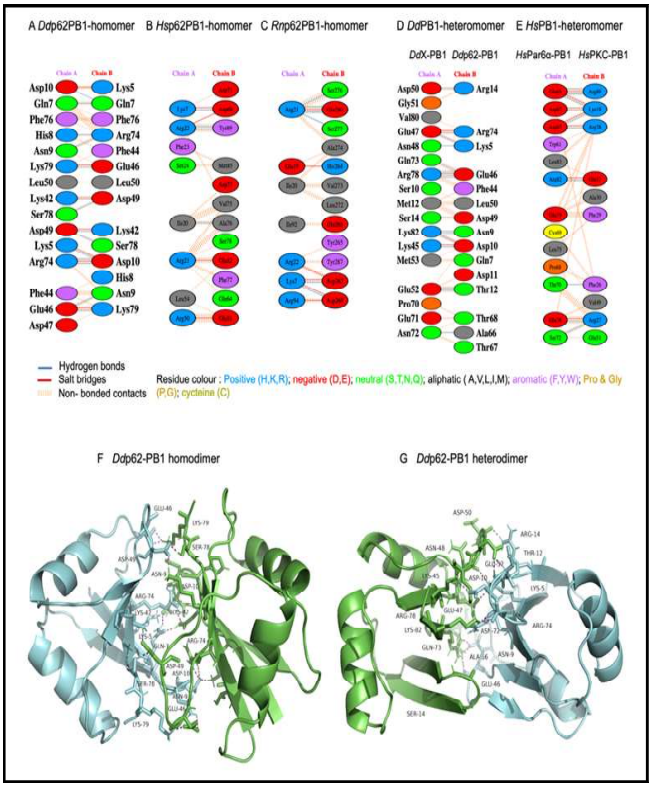

Figure 6: Comparative analysis of interface interactions and polar contacts in different PB1 complexes. Interaction profile of PB1 homodimers of **(A)** *Dictyostelium discoideum* (*de novo* docked), **(B)** *Homo sapiens* (PDB;6JM4) **(C)** *Rattus norvegicus* (PDB; 2KTR) and PB1 heterodimers of **(D)** *Dictyostelium discoideum* (*de novo* docked) **(E)** *Homo sapiens* (PDB;1WMH) generated by PDBsum Generate tool. Interaction maps displaying hydrogen bonds (blue lines), salt bridges (red lines), and non-bonded contacts (dashed lines) between key residues of homodimeric and heterodimeric complexes. Interface residues are colour-coded based on their chemical properties. **(F–G)** Structural representations of the *Dd*p62-PB1 homodimer and heterodimer complexes highlight polar interactions contributing to complex stability.

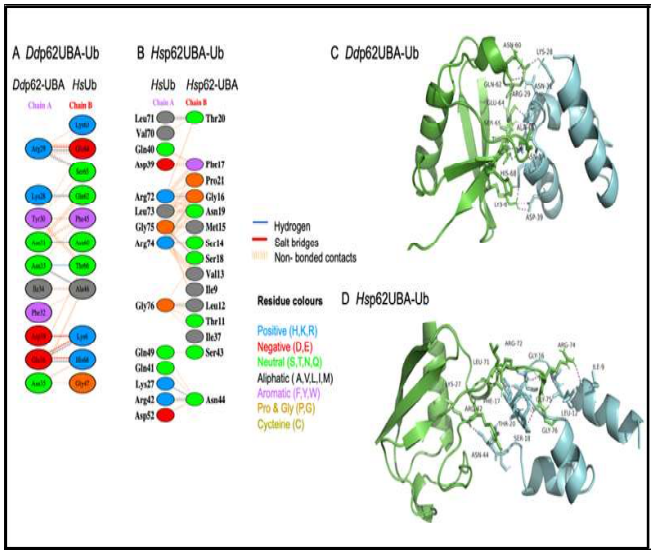

Figure 7:Comparative analysis of interface interactions and polar contacts in p62-UBA domain and Ub (ubiquitin monomer) complex of *Dictyostelium discoideum* and *Homo sapiens*. Interaction profile of UBA (Ubiquitin-Associated) domain of **(A)** *Dd*p62 and **(B)** *Hs*p62 with ubiquitin monomer (*Homo sapiens*, PDB;1UBQ) generated using PDBsum. Interaction maps highlighting hydrogen bonds (blue lines), salt bridges (red lines), and non-bonded contacts (dashed orange lines) between key residues and interface residues are colour-coded based on their chemical properties. **(C–D)** Cartoon representations of *Dd*p62UBA-Ub and *Hs*p62UBA-Ub complexes, showing key polar interactions.

ubiquitin signals, such as K48- and K63-linked polyubiquitin chains, which regulate proteasomal degradation and autophagy, respectively.[55,56] In contrast, the lower eukaryotic counterpart may interact with ubiquitin more rigidly and specifically, less optimised for different ubiquitin modifications.[47,57] This evolutionary divergence highlights the transition of p62 from a primarily oligomerisation-driven scaffold in *Dictyostelium* to a more versatile signalling adaptor in higher eukaryotes, facilitating dynamic regulation of cellular homeostasis.[58]

CONCLUSIONS

This study highlights the evolutionary transition of p62/SQSTM1 from a rigid, aggregation-prone scaffold in lower eukaryotes to a multifunctional signalling adaptor in higher organisms. In *Dictyostelium*, p62 primarily supports protein sequestration and autophagy through strong PB1-mediated oligomerisation and stable ubiquitin interactions, reflecting its role in primitive proteostasis mechanisms. In contrast, the structure of human p62 has evolved towards more flexibility to accommodate more binding partners for regulating pathways like autophagy, oxidative stress response, and NF-κB signalling through additional motifs and a more selective ubiquitin-binding interface. This shift in structure and the function of p62 from rigid oligomer formation to more dynamic scaffold network formation indicates an adaptation towards increasing cellular complexity. These findings provide a better understanding of how the architecture of protein evolves to meet the cellular complexity of organisms and shape the functional diversification across species.

AUTHOR CONTRIBUTIONS

S.G designed and performed the experiments. S.G and S.S analysed the data and wrote the manuscript. Both the authors reviewed and approved the final version of the manuscript.

CONFLICT OF INTEREST

The authors declare that they have no conflict of interest.

REFERENCES

1. **Pankiv, S., Clausen, T. H., Lamark, T., Brech, A., Bruun, J. A., Outzen, H., ... & Johansen, T. 2007.** p62/SQSTM1 binds directly to Atg8/LC3 to facilitate degradation of ubiquitinated protein aggregates by autophagy. *Journal of biological chemistry*, **282(33):** 24131-24145.

2. **Berkamp, S., Mostafavi, S., & Sachse, C. 2021.** Structure and function of p62/SQSTM1 in the emerging framework of phase separation. *The FEBS journal*, **288(24):** 6927-6941.

3. **Geisler, S., Holmström, K. M., Skujat, D., Fiesel, F. C., Rothfuss, O. C., Kahle, P. J., & Springer, W. 2010.** PINK1/Parkin-mediated mitophagy is dependent on VDAC1 and p62/SQSTM1. *Nature cell biology*, **12(2):** 119-131.

4. **Manley, S., Williams, J. A., & Ding, W. X. 2013.** Role of p62/SQSTM1 in liver physiology and pathogenesis. *Experimental biology and medicine*, **238(5):** 525-538.

5. **Romeo, M. A., Montani, M. S. G., Benedetti, R., Arena, A., Gaeta, A., & Cirone, M. 2022.** The dysregulation of autophagy and ER stress induced by HHV-6A infection activates pro-inflammatory pathways and promotes the release of inflammatory cytokines and cathepsin S by CNS cells. *Virus Research*, **313:** 198726.

6. **Manastireanu, D. M., Salazar, N. A., Bejarano, E., & Nieto-Torres, J. L. 2024.** Selective autophagy: a therapeutic target for healthy aging?. *Aging Advances*, **1(1):** 2-22.

7. **Christian, F., Krause, E., Houslay, M. D., & Baillie, G. S. 2014.** PKA phosphorylation of p62/SQSTM1 regulates PB1 domain interaction partner binding. *Biochimica et Biophysica Acta (BBA)-Molecular Cell Research*, **1843(11):** 2765-2774.

8. **Lamark, T., Perander, M., Outzen, H., Kristiansen, K., Øvervatn, A., Michaelsen, E., ... & Johansen, T. 2003.** Interaction codes within the family of mammalian Phox and Bem1p domain-containing proteins. *Journal of Biological Chemistry*, **278(36):** 34568-34581.

9. **Sanz, L., Diaz Meco, M. T., Nakano, H., & Moscat, J. 2000.** The atypical PKC interacting protein p62 channels NF κB activation by the IL 1–TRAF6 pathway. *The EMBO journal*.

10. **Moscat, J., Diaz-Meco, M. T., Albert, A., & Campuzano, S. 2006.** Cell signaling and function organized by PB1 domain interactions. *Molecular cell*, **23(5):** 631-640.

11. **Dao, T. P., Yang, Y., Presti, M. F., Cosgrove, M. S., Hopkins, J. B., Ma, W., ... & Castañeda, C. A. 2022.** Mechanistic insights into enhancement or inhibition of phase separation by different polyubiquitin chains. *EMBO reports*, **23(8):** e55056.

12. **Yan, H., Qi, A., Lu, Z., You, Z., Wang, Z., Tang, H., ... & Wang, H. 2024.** Dual roles of AtNBR1 in regulating selective autophagy via liquid-liquid phase separation and recognition of non-ubiquitinated substrates in Arabidopsis. *Autophagy*, **20(12):** 2804-2815.

13. **Foster, A. D., & Rea, S. L. 2020.** The role of sequestosome 1/p62 protein in amyotrophic lateral sclerosis and frontotemporal dementia pathogenesis. *Neural regeneration research*, **15(12):** 2186-2194.

14. **Duran, A., Linares, J. F., Galvez, A. S., Wikenheiser, K., Flores, J. M., Diaz-Meco, M. T., & Moscat, J. 2008.** The signaling adaptor p62 is an important NF-κB mediator in tumorigenesis. *Cancer cell*, **13(4):** 343-354.

15. **Sánchez-Martín, P., & Komatsu, M. 2018.** p62/SQSTM1–steering the cell through health and disease. *Journal of cell science*, **131(21):** jcs222836.

16. **Lin, X., Li, S., Zhao, Y., Ma, X., Zhang, K., He, X., & Wang, Z. 2013.** Interaction domains of p62: a bridge between p62 and selective autophagy. *DNA and cell biology*, **32(5):** 220-227.

17. **Laurin, N., Brown, J. P., Morissette, J., & Raymond, V. 2002.** Recurrent mutation of the gene encoding sequestosome 1 (SQSTM1/p62) in Paget disease of bone. *The American Journal of Human Genetics*, **70(6):** 1582-1588.

18. **Isogai, S., Morimoto, D., Arita, K., Unzai, S., Tenno, T., Hasegawa, J., ... & Tochio, H. 2011.** Crystal structure of the ubiquitin-associated (UBA) domain of p62 and its interaction with ubiquitin. *Journal of Biological Chemistry*, **286(36):** 31864-31874.

19. **Calvo-Garrido, J., & Escalante, R. 2010.** Autophagy dysfunction and ubiquitin-positive protein aggregates in Dictyostelium cells lacking Vmp1. *Autophagy*, **6(1):** 100-109.

20. **Calvo-Garrido, J., Carilla-Latorre, S., Kubohara, Y., Santos-Rodrigo, N., Mesquita, A., Soldati, T., ... & Escalante, R. 2010.** Autophagy in Dictyostelium: genes and pathways, cell death and infection. *Autophagy*, **6(6):** 686-701.

21. **Jumper, J., Evans, R., Pritzel, A., Green, T., Figurnov, M., Ronneberger, O., ... & Hassabis, D. 2021.** Highly accurate protein structure prediction with AlphaFold. *nature*, **596(7873):** 583-589.

22. **UniProt Consortium. 2023.** UniProt: the Universal Protein Knowledgebase in 2023. Nucleic acids research, **51(D1):** D523–D531. https://doi.org/10.1093/nar/gkac1052

23. **Tamura, K., Stecher, G., & Kumar, S. 2021.** MEGA11: molecular evolutionary genetics analysis version 11. *Molecular biology and evolution*, **38(7):** 3022-3027.

24. **Zdobnov, E. M., Kuznetsov, D., Tegenfeldt, F., Manni, M., Berkeley, M., & Kriventseva, E. V. 2021.** OrthoDB in 2020: evolutionary and functional annotations of orthologs. *Nucleic acids research*. **49(D1):** D389-D393.

25. **Blum, M., Chang, H. Y., Chuguransky, S., Grego, T., Kandasaamy, S., Mitchell, A., ... & Finn, R. D. 2021.** The InterPro protein families and domains database: 20 years on. *Nucleic acids research*, **49(D1):** D344-D354.

26. **Bailey, T. L., Boden, M., Buske, F. A., Frith, M., Grant, C. E., Clementi, L., ... & Noble, W. S. 2009.** MEME SUITE: tools for motif discovery and searching. *Nucleic acids research*, **37(suppl_2):** W202-W208.

27. **Szklarczyk, D., Kirsch, R., Koutrouli, M., Nastou, K., Mehryary, F., Hachilif, R., ... & Von Mering, C. 2023.** The STRING database in 2023: protein–protein association networks and functional enrichment analyses for any sequenced genome of interest. *Nucleic acids research*, **51(D1):** D638-D646.

28. **Abraham, M. J., Murtola, T., Schulz, R., Páll, S., Smith, J. C., Hess, B., & Lindahl, E. 2015.** GROMACS: High performance molecular simulations through multi-level parallelism from laptops to supercomputers. *SoftwareX*, **1:** 19-25.

29. **Heo, L., Park, H., & Seok, C. 2013.** GalaxyRefine: Protein structure refinement driven by side-chain repacking. *Nucleic acids research*, **41(W1):** W384-W388.

30. **Laskowski, R. A., MacArthur, M. W., Moss, D. S., & Thornton, J. M. 1993.** PROCHECK: a program to check the stereochemical quality of protein structures. *Applied Crystallography*, **26(2):** 283-291.

31. **Laskowski, R. A., Jabłońska, J., Pravda, L., Vařeková, R. S., & Thornton, J. M. 2018.** PDBsum: Structural summaries of PDB entries. *Protein science*. **27(1):** 129-134.

32. **Baek, M., Park, T., Heo, L., Park, C., & Seok, C. 2017.** GalaxyHomomer: a web server for protein homo-oligomer structure prediction from a monomer sequence or structure. *Nucleic acids research*, **45(W1):** W320-W324.

33. **Park, T., Won, J., Baek, M., & Seok, C. 2021.** GalaxyHeteromer: protein heterodimer structure prediction by template-based and ab initio docking. *Nucleic Acids Research*, **49(W1):** W237-W241.

34. **Park, T., Baek, M., Lee, H., & Seok, C. 2019.** GalaxyTongDock: Symmetric and asymmetric ab initio protein–protein docking web server with improved energy parameters. *Journal of computational chemistry*, **40(27):** 2413-2417.

35. **Honorato, R. V., Trellet, M. E., Jiménez-García, B., Schaarschmidt, J. J., Giulini, M., Reys, V., ... & Bonvin, A. M. 2024.** The HADDOCK2. 4 web server for integrative modeling of biomolecular complexes. *Nature protocols*, **19(11):** 3219-3241.

36. **Vangone, A., Rodrigues, J. P. G. L. M., Xue, L. C., Van Zundert, G. C. P., Geng, C., Kurkcuoglu, Z., ... & Bonvin, A. M. J. J. 2017.** Sense and simplicity in HADDOCK scoring: Lessons from CASP CAPRI round 1. *Proteins: Structure, Function, and Bioinformatics*, **85(3):** 417-423.

37. **Sanz, L., Sanchez, P., Lallena, M. J., Diaz Meco, M. T., & Moscat, J. 1999.** The interaction of p62 with RIP links the atypical PKCs to NF κB activation. *The EMBO journal*.

38. **Komatsu, M., Kurokawa, H., Waguri, S., Taguchi, K., Kobayashi, A., Ichimura, Y., ... & Yamamoto, M. 2010.** The selective autophagy substrate p62 activates the stress responsive transcription factor Nrf2 through inactivation of Keap1. *Nature cell biology*, **12(3):** 213-223.

39. **Wooten, M. W., Geetha, T., Seibenhener, M. L., Babu, J. R., Diaz-Meco, M. T., & Moscat, J. 2005.** The p62 scaffold regulates nerve growth factor-induced NF-κB activation by influencing TRAF6 polyubiquitination. *Journal of Biological Chemistry*, **280(42):** 35625-35629.

40. **Birgisdottir, Å. B., Lamark, T., & Johansen, T. 2013.** The LIR motif–crucial for selective autophagy. *Journal of cell science*, **126(15):** 3237-3247.

41. **Cheng, M., Li, M., Zhang, Y., Gu, X., Gao, W., Zhang, S., & Liu, J. 2025.** Exploring the mechanism of PPCPs on human metabolic diseases based on network toxicology and molecular docking. *Environment International*, 109324.

42. **Long, J., Gallagher, T. R., Cavey, J. R., Sheppard, P. W., Ralston, S. H., Layfield, R., & Searle, M. S. 2008.** Ubiquitin recognition by the ubiquitin-associated domain of p62 involves a novel conformational switch. *Journal of Biological Chemistry*, **283(9):** 5427-5440.

43. **Vijay-Kumar, S., Bugg, C. E., & Cook, W. J. 1987.** Structure of ubiquitin refined at 1.8 Åresolution. *Journal of molecular biology*, **194(3):** 531-544.

44. **Achudhan, A. B., Kannan, P., & Saleena, L. M. 2023.** Functional metagenomics uncovers nitrile-hydrolysing enzymes in a coal metagenome. *Frontiers in Molecular Biosciences*, **10:** 1123902.

45. **Masum, M. H. U., Rajia, S., Bristi, U. P., Akter, M. S., Amin, M. R., Shishir, T. A., ... & Saha, O. 2023.** *In silico* functional characterization of a hypothetical protein from *Pasteurella multocida* reveals a novel S-Adenosylmethionine-dependent methyltransferase activity. *Bioinformatics and Biology Insights*, **17:** 11779322231184024.

46. **Wilson, M. I., Gill, D. J., Perisic, O., Quinn, M. T., & Williams, R. L. 2003.** PB1 domain-mediated heterodimerization in NADPH oxidase and signaling complexes of atypical protein kinase C with Par6 and p62. *Molecular cell*, **12(1):** 39-50.

47. **Svenning, S., Lamark, T., Krause, K., & Johansen, T. 2011.** Plant NBR1 is a selective autophagy substrate and a functional hybrid of the mammalian autophagic adapters NBR1 and p62/SQSTM1. *Autophagy*, **7(9):** 993-1010.

48. **Sumimoto, H., Kamakura, S., & Ito, T. 2007.** Structure and function of the PB1 domain, a protein interaction module conserved in animals, fungi, amoebas, and plants. *Science's STKE*, **2007(401):** re6-re6.

49. **Pace, C. N., Scholtz, J. M., & Grimsley, G. R. 2014.** Forces stabilizing proteins. *FEBS letters*, **588(14)**, 2177-2184.

50. **Lim, D., Lee, H. S., Ku, B., Shin, H. C., & Kim, S. J. 2019.** Oligomer model of PB1 domain of p62/SQSTM1 based on crystal structure of homo-dimer and calculation of helical characteristics. *Molecules and cells*, **42(10):** 729-738.

51. **Hirano, Y., Yoshinaga, S., Takeya, R., Suzuki, N. N., Horiuchi, M., Kohjima, M., ... & Inagaki, F. 2005.** Structure of a cell polarity regulator, a complex between atypical PKC and Par6 PB1 domains. *Journal of Biological Chemistry*, **280(10):** 9653-9661.

52. **Saio, T., Yokochi, M., Kumeta, H., & Inagaki, F. 2010.** PCS-based structure determination of protein–protein complexes. *Journal of biomolecular NMR*, **46:** 271-280.

53. **Ausaf Ali, S., Imtaiyaz Hassan, M., Islam, A., & Ahmad, F. 2014.** A review of methods available to estimate solvent-accessible surface areas of soluble proteins in the folded and unfolded states. *Current Protein and Peptide Science*, **15(5):** 456-476.

54. **Jakobi, A. J., Huber, S. T., Mortensen, S. A., Schultz, S. W., Palara, A., Kuhm, T., ... & Sachse, C. 2020.** Structural basis of p62/SQSTM1 helical filaments and their role in cellular cargo uptake. *Nature communications*, **11(1):** 440.

55. **Bjørkøy, G., Lamark, T., & Johansen, T. 2006.** p62/SQSTM1: a missing link between protein aggregates and the autophagy machinery. *Autophagy*, **2(2):** 138-139.

56. **Liu, W. J., Ye, L., Huang, W. F., Guo, L. J., Xu, Z. G., Wu, H. L., ... & Liu, H. F. 2016.** p62 links the autophagy pathway and the ubiqutin–proteasome system upon ubiquitinated protein degradation. *Cellular & molecular biology letters*, **21:** 1-14.

57. **Mizushima, N., & Levine, B. 2010.** Autophagy in mammalian development and differentiation. *Nature cell biology*, **12(9):** 823-830.

58. **Johansen, T., & Lamark, T. 2011.** Selective autophagy mediated by autophagic adapter proteins. *Autophagy*, **7(3):** 279-296.

***